British Journal of Pharmacology

DOI:10.1111/j.1476-5381.2012.01993.x
www.brjpharmacol.org

RESEARCH PAPER

AMP-activated protein kinase (AMPK)–dependent and –independent pathways regulate hypoxic inhibition of transepithelial Na^+ transport across human airway epithelial cells

CD Tan[1], RT Smolenski[2], MI Harhun[1], HK Patel[1], SG Ahmed[3], K Wanisch[3], RJ Yáñez-Muñoz[3] and DL Baines[1]

[1]*Pharmacology and Cell Physiology Research Group, Division of Biomedical Sciences, St George's University of London, Cranmer Terrace, London, UK,* [2]*Department of Biochemistry, Medical University of Gdansk, Gdansk, Poland, and* [3]*School of Biological Sciences, Royal Holloway, University of London, Egham, Surrey, UK*

Correspondence
Professor Deborah L Baines, Pharmacology and Cell Physiology Research Group, Division of Biomedical Sciences, St George's University of London, Cranmer Terrace, London, SW17 0RE, UK. E-mail: d.baines@sgul.ac.uk

Keywords
AMPK; ROS; airway; epithelium; Na^+K^+ ATPase; ENaC

Received
11 January 2012
Revised
6 March 2012
Accepted
11 March 2012

BACKGROUND AND PURPOSE

Pulmonary transepithelial Na^+ transport is reduced by hypoxia, but in the airway the regulatory mechanisms remain unclear. We investigated the role of AMPK and ROS in the hypoxic regulation of apical amiloride-sensitive Na^+ channels and basolateral Na^+K^+ ATPase activity.

EXPERIMENTAL APPROACH

H441 human airway epithelial cells were used to examine the effects of hypoxia on Na^+ transport, AMP : ATP ratio and AMPK activity. Lentiviral constructs were used to modify cellular AMPK abundance and activity; pharmacological agents were used to modify cellular ROS.

KEY RESULTS

AMPK was activated by exposure to 3% or 0.2% O_2 for 60 min in cells grown in submerged culture or when fluid (0.1 $mL \cdot cm^{-2}$) was added to the apical surface of cells grown at the air–liquid interface. Only 0.2% O_2 activated AMPK in cells grown at the air–liquid interface. AMPK activation was associated with elevation of cellular AMP : ATP ratio and activity of the upstream kinase LKB1. Hypoxia inhibited basolateral ouabain-sensitive I_{sc} ($I_{ouabain}$) and apical amiloride-sensitive Na^+ conductance (G_{Na+}). Modification of AMPK activity prevented the effect of hypoxia on $I_{ouabain}$ (Na^+K^+ ATPase) but not apical G_{Na+}. Scavenging of superoxide and inhibition of NADPH oxidase prevented the effect of hypoxia on apical G_{Na+} (epithelial Na^+ channels).

CONCLUSIONS AND IMPLICATIONS

Hypoxia activates AMPK-dependent and -independent pathways in airway epithelial cells. Importantly, these pathways differentially regulate apical Na^+ channels and basolateral Na^+K^+ ATPase activity to decrease transepithelial Na^+ transport. Luminal fluid potentiated the effect of hypoxia and activated AMPK, which could have important consequences in lung disease conditions.

Abbreviations

AICAR, 5-aminoimidazole-4-carboxamide-1-β-D-ribofuranoside; AMPK, AMP-activated protein kinase; CaMKK, Ca^{2+}/calmodulin kinase kinase; ENaC, epithelial sodium channel; G_{Na+}, amiloride-sensitive apical conductance; $I_{amiloride}$, amiloride-sensitive transepithelial I_{sc}; $I_{ouabain}$, ouabain-sensitive basolateral current; I_{sc}, short circuit current; LKB1, liver kinase B1; NAC, N-acetylcysteine; NOX, NADPH oxidase; R_t, transepithelial resistance; TAK1, TGF-β-activated kinase 1; TEMPOL, nitrox 2,2,6,6-tetramethylpiperdin-l-yloxy; V_t, transepithelial potential

Introduction

Exposure of the lung to decreased oxygen (e.g. at high altitude or during pathophysiological disorders) is associated with formation of pulmonary oedema (Mairbaurl, 2006). Individuals exposed to high altitude have decreased nasal potential difference, which is indicative of reduced transepithelial transport in the airway (Sartori *et al.*, 2002; Guney *et al.*, 2007). Active vectorial transport of Na^+ across the lung epithelium drives fluid re-absorption, and this serves an essential role in the maintenance of the pericilliary fluid layer volume in the airway and the prevention and resolution of pulmonary oedema in the alveolar region (Hummler *et al.*, 1996; Widdicombe, 2002; Mairbaurl, 2006; Tarran, 2008; Zhou *et al.*, 2008). This process requires the activity of apical amiloride-sensitive Na^+ channels and the basolateral Na^+K^+ ATPase. *In vitro*, exposure to hypoxia inhibited amiloride-sensitive $^{22}Na^+$ influx and Na^+K^+ ATPase activity in human alveolar A549 and rat alveolar type II cells and a role for ROS in regulating these processes was identified (Mairbaurl *et al.*, 1997; Planes *et al.*, 1997; 2002; Wodopia *et al.*, 2000; Dada *et al.*, 2003; Dada and Sznajder, 2007).

More recently, adenosine AMP-activated protein kinase (AMPK) has been shown to play a role in sensing and mediating the effects of hypoxia in a number of tissues by responding to changes in cellular energy balance (Evans *et al.*, 2005; Wyatt *et al.*, 2007). It is a heterotrimeric protein complex consisting of a catalytic α subunit and regulatory β and γ subunits (Winder *et al.*, 1997; Hardie and Sakamoto, 2006). An increase in the cellular AMP : ATP ratio stimulates AMPK activity through the binding of AMP to CBS domains present in the γ subunit (Mortimer *et al.*, 2004). This makes AMPK a better substrate for phosphorylation by upstream kinases such as liver kinase B1 (LKB1)(Wilson *et al.*, 1996; Sutherland *et al.*, 2003; Woods *et al.*, 2003), Ca^{2+}/calmodulin kinase kinase (CaMKK) (Hawley *et al.*, 2005; Woods *et al.*, 2005) and TGF-β-activated kinase 1 (TAK1) (Momcilovic *et al.*, 2006; Xie *et al.*, 2006), while reducing its dephosphorylation by protein phosphatases PP2A and PP2C (Hawley *et al.*, 1996; Marley *et al.*, 1996; Zhao *et al.*, 2007). It has also been proposed that AMPK can be activated independently of changes in the AMP : ATP ratio by changes in mitochondrial ROS, elevation of intracellular Ca^{2+} and increased phosphorylation by CaMKK (Verhoeven *et al.*, 1995; Woods *et al.*, 2005). Once activated, AMPK inhibits ATP-consuming processes and increases ATP-generating processes.

We have shown that pharmacological activation of AMPK decreases transepithelial Na^+ transport across H441 airway epithelial cell monolayers via inhibition of apical amiloride-sensitive Na^+ channels and the activity of Na^+K^+ ATPase (Carattino *et al.*, 2005; Woollhead *et al.*, 2005; 2007; Albert *et al.*, 2008; Gusarova *et al.*, 2009). Hypoxia was recently shown to decrease Na^+K^+ ATPase abundance in the alveolar cell membrane via a pathway involving AMPK and ROS (Gusarova *et al.*, 2009). However, how hypoxia inhibits Na^+ transport pathways in the airway has not been explored. In particular, it is unclear whether AMPK mediates the effects of hypoxia on apically localized amiloride-sensitive Na^+ channels.

We used three different H441 cell culture models for this study as we wanted to compare the responses to hypoxia of air–liquid interface cultures (a physiologically relevant model of the airway) with those of submerged cells cultured on plastic, because much of the published data on the effects of hypoxia use the latter. As transepithelial transport can only be measured in cells grown on permeable supports, we also investigated responses in polarized airway epithelial cells 'submerged' by placing fluid on the apical surface (liquid–liquid interface cultures). Using these models, we investigated the role of AMPK in hypoxia-induced functional changes in transepithelial Na^+ transport across H441 human airway epithelial cell monolayers.

Methods

H441 cell culture

The human lung epithelial cell line, H441, was obtained from the American Type Culture Collection (ATCC) (Manassas, VA). Cells were maintained in RPMI-1640 medium with 10% FBS, 2 mM L-glutamine, 1 mM sodium pyruvate (Sigma, Poole, UK), 5 $\mu g \cdot mL^{-1}$ insulin, 5 $\mu g \cdot mL^{-1}$ transferrin, 10 nM sodium selinite and 100 $U \cdot mL^{-1}$ penicillin, 100 $\mu g \cdot mL^{-1}$ streptomycin and incubated in a humidified atmosphere with 21% O_2 + 5% CO_2 buffered with N_2 (control) at 37°C. Polarized resistive H441 monolayers were cultured on Snapwell clear membranes (Corning, UK) as previously described (Woollhead *et al.*, 2005). Serum was replaced with 4% charcoal stripped FBS, 10 nM tri-iodothyronine (T3) and 200 nM dexamethasone (Sigma) to promote polarization. Cells were maintained for 7–14 days at the air–liquid interface before experimentation. A549 alveolar epithelial cells were cultured in DMEM supplemented with 10% FBS, 2 mM L-glutamine and antibiotics (penicillin/streptomycin). Unless otherwise stated, all cell culture media and supplements were purchased from Invitrogen (Paisley, UK).

Hypoxic treatment

Non-polarized H441 cells grown in submerged culture were seeded onto 6- or 12-well plates. When cells were 90% con-

fluent, the volume of medium overlying the cells was reduced to 0.1 mL·cm^{-2} as described by Planes *et al*. (1997) to decrease the gradient for oxygen diffusion before exposure to a humidified atmosphere containing 0.2% O_2 + 5% CO_2 buffered with N_2 (0.2% O_2) or 3% O_2 + 5% CO_2 buffered with N_2 (3% O_2) at 37°C for 15 or 30 or 60 min. Polarized H441 cells cultured on permeable supports at the air–liquid interface were exposed to a humidified atmosphere containing 0.2% O_2 + 5% CO_2 buffered with N_2 (0.2% O_2) or 3% O_2 + 5% CO_2 buffered with N_2 (3% O_2) at 37°C for 15 or 30 or 60 min. Liquid–liquid interface experiments were conducted with 0.1 mL·cm^{-2} PSS added to the apical chamber before exposure to hypoxia as described above. Cells were pretreated with STO609 (Sigma) 25 μM for 30 min, geldenamycin (Enzo Life Sciences, Exeter, UK) 10 μM for 24 h and ionomycin (Merck, Nottingham, UK) 1 μM for 15 min.

Fluo-3 fluorescence imaging

H441 cells were seeded onto glass coverslips forming the bottom of experimental chambers (as submerged cultures). Cells were loaded with 2 μM Ca^{2+}-sensitive fluorescent indicator fluo-3AM (Invitrogen) for 1 h at 37°C in culture medium also containing a non-ionic detergent Pluronic F127 (0.002%) and an inhibitor of organic cation extrusion systems probenecid (2.5 mM). The cells accumulated very little of the dye unless two latter compounds were present (McAlroy *et al*., 2000). Fluo-3 fluorescence was recorded using *x–y* time series mode of an LSM 510 laser-scanning confocal microscope (Carl Zeiss Ltd., Welwyn Garden City, UK) and analysed as previously described (Harhun *et al*., 2006).

Ussing chamber experiments

Ussing chamber experiments were performed as described previously (Ramminger *et al*., 2000; Woollhead *et al*., 2005). H441 cell monolayers were mounted in Ussing chambers and bathed with PSS (mM): NaCl, 117; $NaHCO_3$, 25; KCl, 4.7; $MgSO_4$, 1.2; KH_2PO_4, 1.2; $CaCl_2$, 2.5; D-glucose, 11; pH 7.3–7.4 and equilibrated with pre-mixed gas 0.2% O_2 + 5% CO_2 + 94.8% N_2 (0.2% O_2) or 3% O_2 + 5% CO_2 + 92% N_2 (3% O_2) or 21% O_2 + 5% CO_2 + 74% N_2 (control) maintained at 37°C and continuously circulated throughout the course of the experiment by airlift. Short circuit current (I_{sc}) was measured by clamping transepithelial potential (V_t) at 0 using a DVC1000 current /clamp module (WPI, Hitchin, UK). Every 30 s, a 2 mV potential was applied to enable the calculation of transepithelial resistance (R_t). Amiloride-sensitive transepithelial I_{sc} ($I_{amiloride}$) was measured by adding amiloride (10 μM) to the solution perfusing the apical membrane of the monolayer. Ouabain-sensitive basolateral current ($I_{ouabain}$) was determined by maintaining the epithelial monolayer under the conditions described above and permeabilizing the apical membrane with nystatin (75 μM) to isolate the basolateral current generated by Na^+ K^+ ATPase. Apical permeabilization permits unrestricted movement of monovalent cations across the apical membrane and leads to equilibration of intracellular ion concentrations with external ionic conditions. The increase in intracellular Na^+ leads to increased basolateral pump current. The decrease in peak basolateral current following the application of 1 mM ouabain is indicative of the activity of the Na^+ K^+ ATPase under these experimental conditions. Amiloride-sensitive apical conductance (G_{Na+}), was determined by bathing monolayers in potassium gluconate solution [composition (mM): potassium gluconate, 121.7; $KHCO_3$, 25; $MgSO_4$, 1.2; KH_2PO_4, 1.2; calcium gluconate, 11.5; D-glucose, 11; pH 7.3–7.4]. This was mixed with PSS to give a PSS : potassium gluconate solution ratio of 8.1:91.9 and a final Na^+ concentration of ~11.5 mM (equilibrated with premixed gas as described above). Na^+K^+ ATPase was inhibited with 1 mM ouabain, and the basolateral membrane was permeabilized with 75 μM nystatin. A Na^+ gradient across the apical membrane was then established by raising the concentration of Na^+ in the apical chamber to 55 mM with a sodium gluconate solution [composition (mM): sodium gluconate, 117; $NaHCO_3$, 25; potassium gluconate, 4.7; $MgSO_4$, 1.2; KH_2PO_4, 1.2; calcium gluconate, 2.5; D-glucose, 11; pH 7.3–7.4 (91.9:8.1 with PSS) equilibrated with premixed gas as described above]. Amiloride (10 μM) was added to the apical bath to inhibit currents, and amiloride-sensitive G_{Na+} was estimated from the amiloride-sensitive apical current (I_{ap}) using the equation $G_{Na+} = I_{ap}/V_{Na+}$, where V_{Na+} is the driving force for Na^+ entry where potential difference across the apical membrane (V_a) is clamped at 0 and the equilibrium potential for Na^+ (E_{Na}) = 41.8 mV. The value for E_{Na+} was calculated using the Nernst equation for the ionic conditions applied. There is no driving force for the passive movement of Cl^- across the apical membrane as the PD is held at 0 mV, and the concentrations of Cl^- in the apical/basolateral baths are the same (Collett *et al*., 2002; Richard *et al*., 2004; Woollhead *et al*., 2005; 2007)

Lentiviral vector construction and cell transduction

cDNA encoding for a constitutively active mutant of α-AMPK (CA) was amplified from pcDNA3/AMPKaCA (kind gift of Prof David Carling, Imperial College London, UK) by PCR and subcloned under the control of the CMV promoter into *Xho*I/*Spe*I of the self-inactivating (SIN) (Zufferey *et al*., 1998) lentiviral transfer plasmid pRRLsc_SFFV_eGFP_CMV_NCS1_WPRE, replacing the NCS1 cDNA. AMPKα (CGCAGCAAT AAGCATGCATA) (Myerburg *et al*., 2010) and non-targeting shRNA sequences (Sh-neg: ACTACCGTTGTTATAGGTG) were cloned under the control of the human H1 promoter into *Mlu*I/*Pst*I sites of pRRLsc_CMV_eGFP_WPRE_H1 (pshLENTImax), a SIN lentiviral transfer plasmid for RNAi. Lentiviral transfer plasmids were packaged into third-generation, VSV-G pseudotyped vectors. Briefly, vectors were produced by calcium phosphate-mediated transient transfection of HEK293T. The packaging plasmids were pMDLg/pRRE and pRSV-rev, while pMD2.G provided the VSV-G envelope gene (Dull *et al*., 1998). Cell culture supernatant was harvested 2–3 days post transfection, and vector particles were concentrated by ultracentrifugation. Vectors were titrated in HeLa cells by scoring eGFP fluorescence units using flow cytometry (Yanez-Munoz *et al*., 2006). H441 cells were seeded onto permeable supports. Following overnight incubation, the cells were transduced with lentiviral vectors at an approximate multiplicity of infection (MOI) of 10 for 4 h. The cells were incubated in fresh growth medium overnight, cultured at the air–liquid interface and used for functional studies 96 h after transduction.

Measurement of intracellular adenine nucleotide concentration

The adenine nucleotides ATP, ADP, AMP and TAN (total adenine nucleotides) were measured in untreated monolayers or those exposed to 0.2% O_2 or 3% O_2 for 60 min. Cells were washed with PBS on ice, and then (0.4 M) perchloric acid was added to extract the nucleotides. Cell extracts were neutralized with 3 M K_3PO_4 and analysed by reverse-phase HPLC (Hewlett-Packard 1100 series linked to a diode array detector, ISS Ltd., Dartford, UK) as described previously in detail (Woollhead *et al.*, 2007; Nofziger *et al.*, 2009). Protein content of the perchlorate precipitate was analysed using the Bradford assay (Fisher Scientific UK Ltd., Loughborough, UK).

Western blotting

Cells were lysed in lysis buffer [50 mM Tris–HCl, pH 7.4; 1% NP-40; 0.25% sodium deoxycholate; 150 mM NaCl; 1 mM EDTA; 1 mM EGTA, 1 mM PMSF, 1 mM Na_3VO_4, 50 mM NaF, 5 mM sodium pyrophosphate and 1% (w v^{-1}) Protease inhibitor cocktail]. Cellular debris was removed by centrifugation at 13 000 × *g* for 10 min, and protein concentrations were determined using the Bradford assay (as above). Approximately 30–50 μg of proteins were fractionated on 4–12% Bis–Tris gel (Invitrogen) alongside pre-stained protein standards (Santa Cruz, CA) and transferred onto Hybond-P PVDF Membrane (GE Healthcare, Amersham, UK). Membranes were incubated in TBS-T containing 5% (w v^{-1}) nonfat milk powder for 1 h at room temperature before incubation with primary antibodies; anti-phospho-AMPKα (Thr^{172}), anti-AMPKα, anti-phospho-ACC(Ser^{79}), anti-ACC (Cell Signaling Technology, Danvers, MA) (all diluted 1:1000) or anti-LKB1 (Abcam, Cambridge, UK) (1:500) or anti-β-actin (Abcam) (1:2000), followed by incubation with species-specific HRP-conjugated secondary antisera (Sigma). Immunostained proteins were visualized with SuperSignal west pico chemiluminescent substrate (GE Healthcare). Densitometric quantification was performed using Scion Image (NIH).

Statistical analysis

Statistical analysis was carried out using ANOVA or Student's unpaired or paired *t*-tests where applicable. *P*-values of <0.05 were considered significant. Results are presented as mean ± SEM.

Results

Effect of hypoxia on the intracellular adenine nucleotide concentration

As the cellular AMP : ATP ratio is an important activator of AMPK, we determined whether the AMP : ATP ratio was altered in cells exposed to hypoxia. Cellular extracts from H441 cells monolayers were analysed by HPLC. Exposure of submerged cultures to 3% O_2 for 60 min resulted in an 8 fold increase in the AMP : ATP ratio compared with control ($P < 0.001$, $n = 3$). This was the result of both a decrease in ATP concentration and an increase in AMP concentration ($P < 0.01$, $n = 3$ respectively) (Table 1). In H441 cells grown at the air–liquid interface, exposure to 3% O_2 for an hour did not affect the AMP : ATP ratio ($n = 3$). However, when exposed to 0.2% O_2 the AMP : ATP ratio was approximately fivefold higher than control ($P < 0.001$, $n = 3$) (Table 1).

Effect of hypoxia on the activity of AMPK

In human H441 airway epithelial cells grown in submerged culture, exposure to 3% O_2 significantly increased the phosphorylation of Thr^{172} of the AMPK α-subunit in a time-dependent fashion (pAMPK/tAMPK, $P < 0.05$, $n = 4$). Phosphorylation of Ser^{79} of ACC was also observed to increase with time (Figure 1A and B). Treatment with AICAR, an AMP-mimetic activator of AMPK (2 mM for 60 min), significantly increased phosphorylation of AMPKα in H441 cells ($P < 0.05$, $n = 4$). Phosphorylation of ACC followed a similar pattern (Figure 1A and B).

Table 1

Cellular adenine nucleotide concentration (nmol mg^{-1} cell protein) determined in H441 cells grown in submerged culture or at the air–liquid interface and exposed to 3% or 0.2% O_2 for 60 min

	ATP	ADP	AMP	TAN	ADP : ATP	AMP : ATP
Submerged cultures						
Control	13.8 ± 0.4	0.57 ± 0.05	0.12 ± 0.02	14.5 ± 0.4	0.04 ± 0.002	0.01 ± 0.002
3% O_2	7.2 ± 0.04**	1.37 ± 0.08*	0.56 ± 0.06**	9.1 ± 0.2*	0.19 ± 0.01**	0.08 ± 0.01***
Air–liquid interface cultures						
Control	30.2 ± 0.5	1.38 ± 0.12	0.18 ± 0.01	31.8 ± 0.6	0.046 ± 0.004	0.006 ± 0.001
3% O_2	31.2 ± 0.7	1.38 ± 0.05	0.30 ± 0.01	33.0 ± 0.7	0.044 ± 0.002	0.009 ± 0.001
0.2% O_2	31.1 ± 0.2	1.33 ± 0.12	0.91 ± 0.06***	33.3 ± 0.1	0.043 ± 0.004	0.029 ± 0.001***

Results are shown as mean ± SEM. Significantly different from control: *$P < 0.05$, **$P < 0.01$, ***$P < 0.001$ ($n = 3$). TAN, total adenine nucleotides.

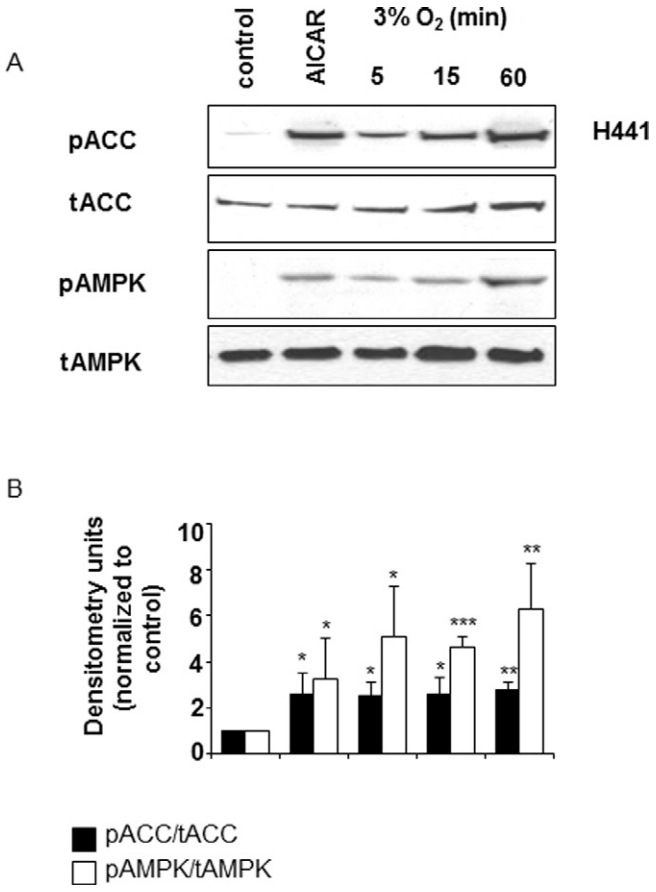

Figure 1

Time course of AMPK activation in H441 cells grown in submerged culture. H441 cells were treated with 2 mM AICAR for 60 min or exposed to 3% O_2 for 5, 15 or 60 min. (A) Typical Western blot of cell extracts immunoblotted for phospho-Ser[79] of ACC (pACC), total ACC (tACC), phospho-Thr[172] of AMPKα (pAMPK) or total AMPKα (tAMPK). (B) Densitometry analysis of protein abundance pAMPK/tAMPK and pACC/tACC from Western blots as shown in (A). Results are shown as mean ± SEM. Significantly different from control: *$P < 0.05$, **$P < 0.01$, ***$P < 0.001$ ($n = 4$).

In monolayers grown at the air–liquid interface, exposure to 3% O_2 for 60 min did not increase the phosphorylation of AMPKα and ACC (phosphoAMPK /totalAMPK and phosphoACC/totalACC) (Figure 2A and C). However, consistent with the observed increase in the AMP : ATP ratio, exposure to 0.2% O_2 for 15 or 60 min significantly elevated phosphorylation of AMPKα ($P < 0.01$, $n = 4$) and ($P < 0.05$, $n = 4$), respectively (Figure 2A–D).

Addition of 0.1 mL·cm^{-2} of PSS to the apical surface increased phosphorylation of AMPK and ACC ($P < 0.05$, $n = 3$, respectively) in cells exposed to 3% O_2. Furthermore, we observed that addition of 0.1 mL·cm^{-2} of fluid to the apical compartment mildly activated AMPK in cells exposed to 21% O_2 (Figure 3A–C). These data indicate that fluid submersion of cells increases sensitivity to hypoxia.

As we wished to investigate the regulation of AMPK activity and whether AMPK mediated effects on Na^+K^+ ATPase and/or apical amiloride-sensitive Na^+ conductance, in all subsequent experiments we only used hypoxic situations in which AMPK was activated. As some drugs needed to be administered to the apical surface for efficacy, these were either cells grown at the air–liquid interface and exposed to 0.2% O_2 or cells exposed to 3% or 0.2% O_2 at the liquid–liquid interface.

Effect of ROS inhibitors on AMPK activity

Under the conditions tested, our data indicated that AMPK was only activated in cells where there was an increase in the AMP : ATP ratio. However, hypoxic elevation of ROS may also contribute to the activation of AMPK. We therefore investigated whether N-acetylcysteine (NAC; a scavenger of H_2O_2) and TEMPOL (a scavenger of superoxide, O_2^-) had any effect on AMPK activity. Pretreatment with NAC (10 μM) had no effect on phosphorylation of AMPKα and ACC ($n = 3$) in cells exposed to 3% or 0.2% O_2 at the liquid–liquid interface (Figure 4A and B). Similarly, TEMPOL (3 mM) had no observable effect on hypoxia-induced phosphorylation of ACC ($n = 2$) (Figure 4C). These data indicate that in H441 cells, activation of AMPK is not dependent on changes in intracellular H_2O_2 or superoxide.

Effect of inhibition of AMPK upstream kinases on hypoxia-induced activation of AMPK

LKB1 and CaMKK are major upstream kinases of AMPK. In some cell types, hypoxia can elevate intracellular Ca^{2+} and activate CaMKK (Gusarova *et al.*, 2011). Therefore, we tested whether CaMKK played a role in the phosphorylation of AMPK in H441 cells after exposure to hypoxia. A brief (2 min) exposure to the Ca^{2+} ionophore ionomycin (1 μM) evoked a robust increase in intracellular Ca^{2+} in H441 cells preloaded with the Ca^{2+} indicator fluo-3AM (Liu and Hermann, 1978). Intracellular Ca^{2+} concentration was restored following washout of ionomycin from extracellular media consistent with findings in other cell types (Clair *et al.*, 2001; Abramov and Duchen, 2003). This indicated that Ca^{2+} uptake by the intracellular stores and Ca^{2+} extrusion from the cells remained viable (Figure 5A and B). However, we were unable to show any changes in intracellular Ca^{2+} concentration after exposure to hypoxia. Treatment with ionomycin for 15 min increased the phosphorylation of AMPKα and ACC in H441 cells grown at the air–liquid interface. The phosphorylation of AMPKα was attenuated by pretreatment with the CaMKK inhibitor STO-609 (Figure 5C). These data indicate that elevation of Ca^{2+} and activation of CaMKK increased AMPK phosphorylation in H441 cells in the absence of metabolic conditions that would alter the AMP : ATP ratio. However, STO609 did not prevent phosphorylation of AMPKα and ACC in cells grown in submerged culture and exposed to 3% O_2 for 60 min (Figure 6A, B and F) or in cells grown at the air–liquid interface and exposed to 0.2% O_2 for 60 min (Figure 6C and D). As a positive control, STO609 inhibited the elevation of phosphorylated AMPKα in human alveolar A549 cells grown in submerged culture and exposed to 3% O_2 (Figure 6E) consistent with the findings of (Gusarova *et al.*, 2011).

There are no specific inhibitors of LKB1. However, LKB1 is associated with Heat shock protein 90 (HSP90) and Cdc37 to

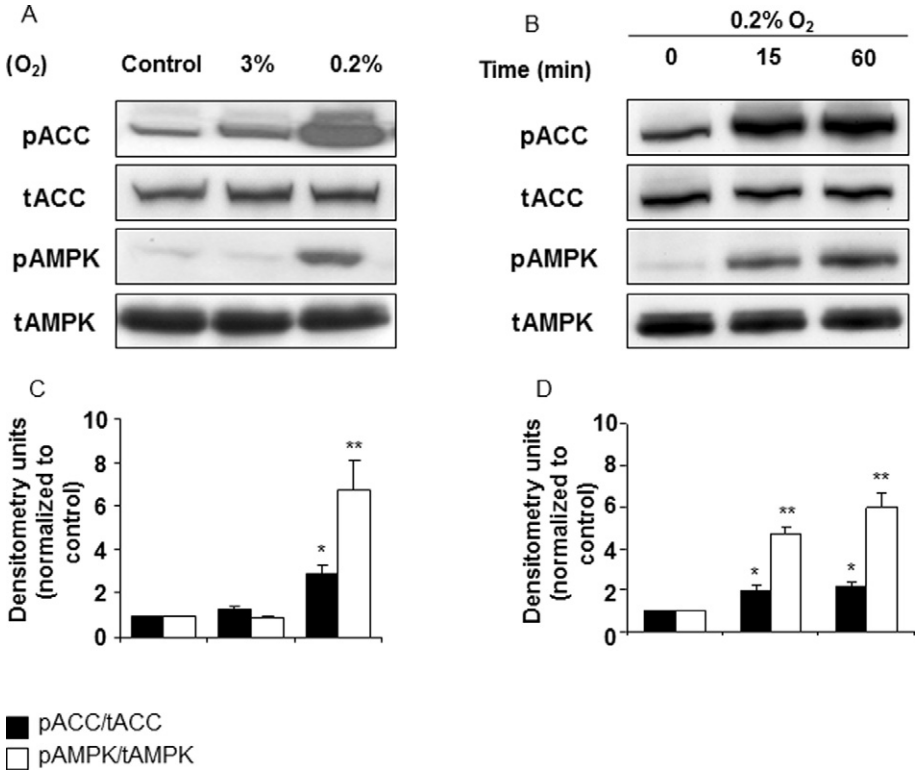

Figure 2

AMPK activation in H441 cells grown at the air–liquid interface. (A) Typical Western blot of extracts from cells grown at the air–liquid interface and maintained at 21% O_2 (control) or exposed to 3% or 0.2% O_2 for 60 min and immunoblotted for phosphor-Ser^{79} of ACC (pACC), total ACC (tACC), phospho-Thr^{172} of AMPKα (pAMPK) or total AMPKα (tAMPK). (B) Typical Western blot of extracts from cells exposed to 0.2% O_2 for 15 or 60 min and immunoblotted for phospho-Ser^{79} of ACC (pACC), total ACC (tACC), phospho-Thr^{172} of AMPKα (pAMPK) or total AMPKα (tAMPK). (C and D) Densitometry analysis of protein abundance pAMPK/ tAMPK and pACC/tACC from Western blots as shown in (A) and (B), respectively. Results are shown as mean ± SEM. Significantly different from control: $^*P < 0.05$, $^{**}P < 0.01$ ($n = 4$).

prevent degradation by the proteosome (Nony *et al.*, 2003; Sutherland *et al.*, 2003). In H441 cells, geldanamycin (10 μM, 24 h), a pharmacological inhibitor of HSP90, markedly decreased LKB1 protein abundance to 40% of control ($P < 0.05$, $n = 3$) (Figure 7A and B) but did not affect total cellular AMPKα or ACC abundance (Figure 7C and D). A decreased LKB1 abundance reduced the phosphorylation of AMPKα in cells grown at the air–liquid interface and exposed to 0.2% O_2 for 60 min when compared with non-geldanamycin-treated cells ($P < 0.05$, $n = 3$). The phosphorylation of ACC was also concomitantly reduced ($P < 0.05$, $n = 3$) (Figure 7C and D). Thus, these data indicate that hypoxia-induced phosphorylation of AMPK in polarised H441 cells is associated with LKB1-mediated phosphorylation.

Effect of hypoxia on transepithelial ion transport processes across H441 cell monolayers

We wanted to determine whether AMPK mediated the effects of hypoxia on transepithelial Na^+ transport processes in H441 cells. Therefore, we investigated monolayers under conditions where AMPK was activated with Ussing chamber experiments performed on polarized H441 cell monolayers at the liquid–liquid interface exposed to 3% or 0.2% O_2 at for 60 min. Cells exposed to 3% and 0.2% O_2 exhibited a significant decrease in transepithelial $I_{amiloride}$ from 20.9 ± 1.7 to 16.6 ± 1.4 μA·cm^{-2} and 12.5 ± 1.4 μA·cm^{-2} ($P < 0.01$, $n = 4$, respectively). $I_{ouabain}$ was reduced from 102.9 ± 10.6 to 82.4 ± 11.8 and 66.4 ± 13.6 μA·cm^{-2} ($P < 0.05$, $n = 4$, respectively) (Figure 8A–C). Amiloride-sensitive G_{Na+} was also significantly reduced from 197 ± 37.4 to 131.3 ± 23.0 and 120 ± 9.8 μS·cm^{-2} ($P < 0.05$, $n = 4$, respectively) (Figure 8D and E). Taken together, these data indicate that under these conditions, exposure to hypoxia inhibits both the apical and basolateral components of transepithelial Na^+ transport. Interestingly, exposure to 0.2% O_2, but not 3% O_2, resulted in a significant increase in the transepithelial resistance from 467.3 ± 39.7 to 536.2 ± 49.2 Ω·cm^2 ($P < 0.01$, $n = 4$).

Effect of AMPK lentiviral vectors on transepithelial Na^+ transport

Transduction of H441 cells grown at the air–liquid interface with lentivector containing a short hairpin sequence specific to AMPKα1/2 (sh-AMPK) resulted in a reduction of total AMPK abundance compared to control lentivector (Sh-negative) (Figure 9A). Exposure to 0.2% O_2 for 60 min resulted in a significant inhibition of $I_{ouabain}$ to 76 ± 7% of control in

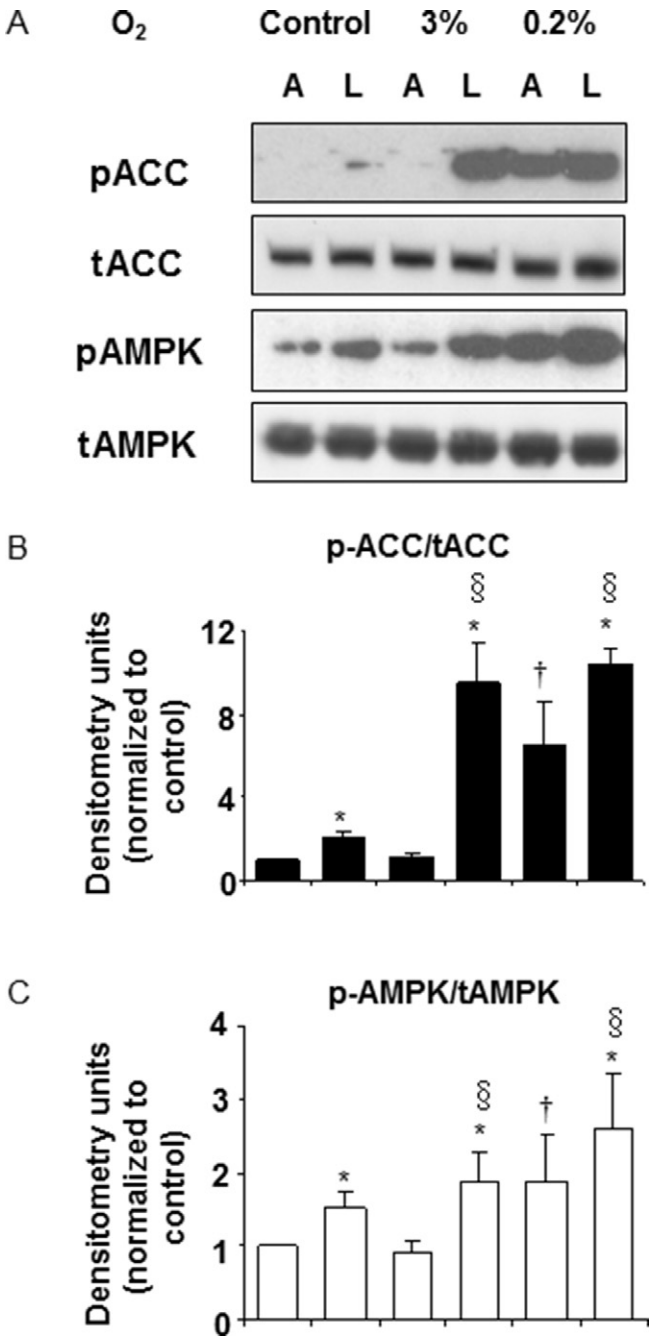

Figure 3

AMPK activation in H441 cell monolayers grown at the air–liquid interface or liquid–liquid interface. (A) Monolayers grown at the air–liquid interface (A) or with 0.1 mL·cm^{-2} added to the apical surface (liquid–liquid interface, L) were maintained at 21% O_2 (control) or exposed to 3% or 0.2% O_2 for 60 min. Typical Western blot of cell extracts immunoblotted for phospho-Ser^{79} of ACC (pACC), total ACC (tACC), phospho-Thr^{172} of AMPKα (pAMPK) or total AMPKα (tAMPK). (B) Densitometry analysis of protein abundance pACC/ tACC. (C) Densitometry analysis of protein abundance pAMPK/tAMPK from Western blots as shown in panel A. Results are shown as mean ± SEM. §Significantly different from control at the air–liquid interface, $P < 0.05$ ($n = 3$); †significantly different from control at the liquid–liquid interface, $P < 0.05$ ($n = 3$); *significantly different from air–liquid interface at the same % O_2, $P < 0.05$ ($n = 3$).

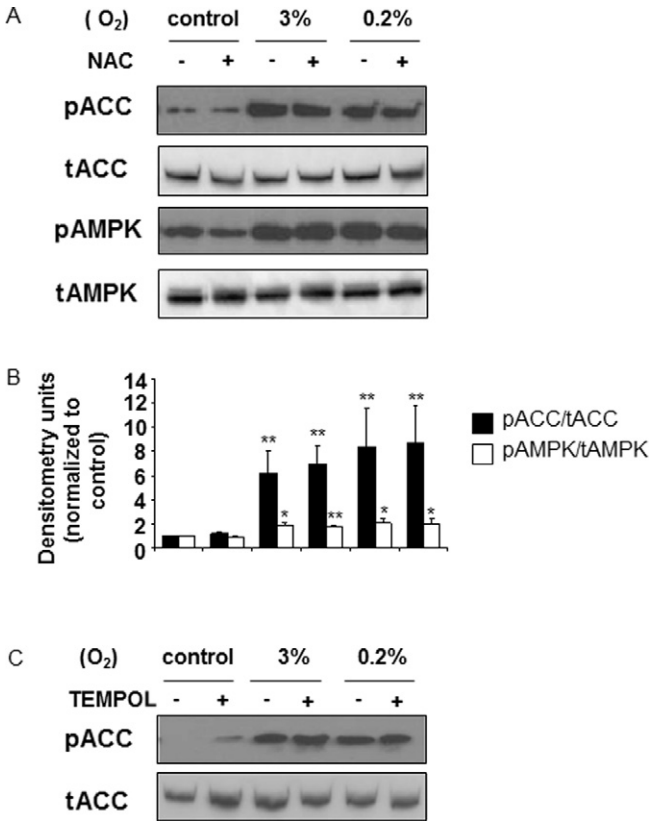

Figure 4

Effect of NAC and TEMPOL on hypoxia-induced AMPK activation. (A) Cells grown at the liquid–liquid interface were maintained at 21% O_2 (control) or exposed to 3% or 0.2% O_2 for 60 min in the presence or absence of NAC. Typical Western blot of cell extracts immunoblotted for phospho-Ser^{79} of ACC (pACC), total ACC (tACC), phospho-Thr^{172} of AMPKα (pAMPK) or total AMPKα (tAMPK). (B) Densitometry analysis of protein abundance pAMPK/ tAMPK and pACC/tACC from Western blots as shown in (A). Results are shown as mean ± SEM. Significantly different from control: *$P < 0.05$, **$P < 0.01$ ($n = 3$). (C) Cells grown at the liquid–liquid interface were maintained at 21% O_2 (control) or exposed to 3% or 0.2% O_2 for 60 min in the presence or absence of TEMPOL. Typical Western blot of cell extracts immunoblotted for phospho-Ser^{79} of ACC (pACC), total ACC (tACC). This blot was repeated with similar results.

Sh-negative transfected cells ($P < 0.05$, $n = 4$) but had no effect in the presence of Sh-AMPK (Figure 9B). Exposure to 0.2% O_2 inhibited G_{Na+} to 60 ± 4 % ($P < 0.01$, $n = 4$) and to 69 ± 9 % ($P < 0.05$, $n = 4$) of control in Sh-negative and Sh-AMPK-treated cells (Figure 9C). Transduction with lentivector containing constitutively active AMPK (CA-AMPK) resulted in expression of CA-AMPK protein in addition to endogenous AMPK in H441 cells (Figure 10A). Under non-hypoxic control conditions, expression of CA-AMPK reduced $I_{ouabain}$ to 70 ± 7% ($P < 0.05$, $n = 4$) of that determined in Sh-negative transfected cells (Figure 10B). Exposure to 0.2% O_2 for 60 min in the presence of CA-AMPK had no further effect ($n = 4$) (Figure 10C). These data support a role for AMPK in mediating the effects of hypoxia on Na^+K^+ ATPase but not apically localized amiloride-sensitive Na^+ channels in H441 cells.

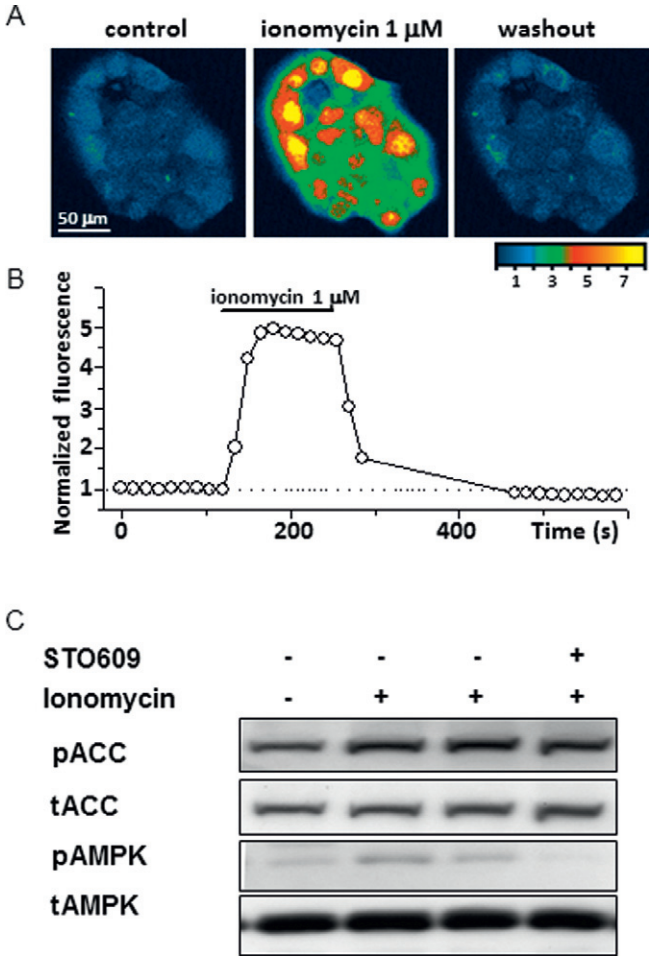

Figure 5

Effect of ionomycin on intracellular Ca^{2+} and activation of AMPK in H441 cells. (A) Representative fluorescent confocal *x–y* images of H441 cells taken before, during and after exposure to 1 µM ionomycin. (B) Plot of the time course of the normalized fluorescence averaged from a group of ~20 H441 cells briefly exposed to ionomycin (1 µM). (C) H441 cells grown at the air–liquid interface were treated with ionomycin (15 min) with or without pretreatment (30 min) with the CaMKK inhibitor STO609 (STO609). Typical Western blots of cell extracts immunoblotted for phospho-Ser^{79} of ACC (pACC), total ACC (tACC), phospho-Thr^{172} of AMPKα (pAMPK) or total AMPKα (tAMPK). These blots were repeated with similar results.

Effect of NAC, TEMPOL and apocynin on apical G_{Na+}

H441 cells grown at the liquid–liquid interface were pretreated with NAC (10 mM) or TEMPOL (3 mM) or apocynin (300 µM) and exposed to 3% or 0.2% O_2 for 60 min. The transepithelial resistance (R_t) in NAC treated cells was 395.5 ± 36.0 Ω cm^2, and this was not significantly affected by exposure to 3% or 0.2% O_2 (487.9 ± 81.5 and 512.5 ± 68.0 Ω cm^2, n = 3, respectively). However, in the presence of NAC, exposure to 3% or 0.2% O_2 inhibited amiloride-sensitive G_{Na+} from 170.4 ± 7.2 to 110.0 ± 10.8 ($P < 0.01$, $n = 3$) and 78.0 ± 2.7 µS cm^{-2} ($P < 0.001$, n = 3), respectively (Figure 11A). The R_t in TEMPOL-treated cells was 403.0 ± 96.0 Ω cm^2 and was also not affected by exposure to 3% or 0.2% O_2 (442.5 ± 91.6 and 430.8 ± 125.8 Ω cm^2, n = 3 respectively). The apical amiloride-sensitive G_{Na+} was reduced by TEMPOL to 50.4 ± 4.7 µS cm^{-2} compared with untreated cells and was not further inhibited by exposure to 3% or 0.2% O_2 for 60 min (30.2 ± 7.7 and 47.9 ± 4.2 µS cm^{-2}, n = 3 respectively) (Figure 11B). In apocynin-treated monolayers, amiloride-sensitive G_{Na+} was 255.0 ± 33.3 18.3 µS cm^{-2}, and exposure to 3% or 0.2% O_2 had no significant effect (251.9 ± 2.1 and 216.8 ± 18.3 µS cm^{-2}, n = 3 respectively) (Figure 11C). Taken together, these data indicate that TEMPOL and apocynin prevented the effect of hypoxia on apical G_{Na+}.

Discussion and conclusions

Exposure to hypoxia activated AMPK in H441 airway and A549 distal lung epithelial cells. However, we found that there was a difference in the response to hypoxia between H441 cells grown in submerged culture or at the liquid–liquid interface and those grown at the air–liquid interface. In cells grown in submerged culture, exposure to 3% O_2 was sufficient to increase the AMP : ATP ratio and activate AMPK, consistent with findings that 3% O_2 activated AMPK in rat alveolar type II cells (Gusarova *et al.*, 2009). In contrast, in cells grown at the air–liquid interface, only 0.2% O_2 increased the AMP : ATP ratio and activated AMPK. Moreover, after exposure to 0.2% O_2, the adenine nucleotide concentrations were comparable with those we have previously published for pharmacological activation of AMPK with phenformin (a mitochondrial inhibitor). Given that mitochondrial PO_2 is approximately 0.4% O_2, it would seem reasonable that exposure to 0.2% O_2 would disrupt mitochondrial function and energy generation. Interestingly, whilst phenformin robustly activated AMPK at 60 min (similar to 0.2% O_2), a 4 h exposure to metformin was required to activate AMPK (Woollhead *et al.*, 2007). Thus, a longer exposure to 3% O_2 may be necessary to elicit changes in the AMP : ATP ratio and activation of AMPK in cells grown at the air–liquid interface.

That apical fluid modified the response to hypoxia was further supported by our finding that the addition of fluid to the apical surface (0.1 mL·cm^{-2}) of cells grown at the air–liquid interface resulted in activation of AMPK by 3% O_2. Thus, the presence of fluid 'sensitizes' the response to reduced PO_2. O_2 is poorly soluble (approx 0.231 mL L^{-1} kPa^{-1}) in aqueous solution, and Fick's law of diffusion predicts that medium between the surface of the cells and the gaseous environment produces a barrier to the diffusion of O_2 to the cell surface and subsequently the mitochondria (Allen *et al.*, 2001). A number of studies have investigated how fluid influences the PO_2 of oxygen near the cell membrane using oxygen electrodes (Metzen *et al.*, 1995; Allen *et al.*, 2001; Bambrick *et al.*, 2011; Lynn *et al.*, 2011). These studies indicate that pericellular PO_2 is lower than the environmental gas PO_2, even in hypoxia. The level of pericellular PO_2 is dependent on fluid depth, the number and type of cells. Thus, if O_2 demand exceeds O_2 diffusion, the pericellular PO_2 falls. It is likely that both proliferating H441 cells and those at the liquid–liquid interface, which are actively transporting ions, have high O_2 demand (Metzen *et al.*, 1995). Therefore, the apical pericellular PO_2 of cells in submerged culture could be

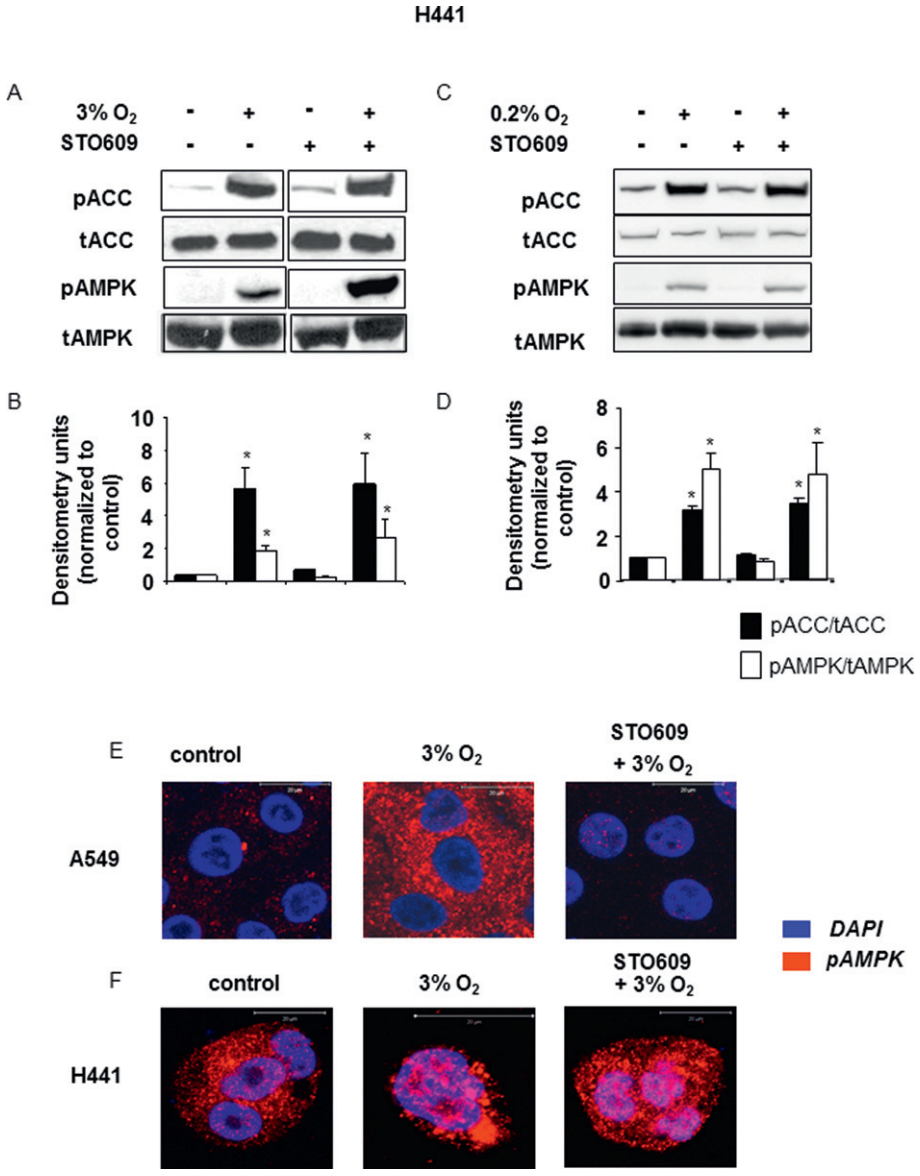

Figure 6

Effect of STO609 on activation of AMPK in H441 cells exposed to hypoxia. (A) Typical Western blots of cell extracts from H441 cells grown at the liquid–liquid interface, with or without pretreatment with the CaMKK inhibitor STO609 and maintained at 21% O_2 (control) or exposed to 3% for 60 min and immunoblotted for phospho-Ser[79] of ACC (pACC), total ACC (tACC), phospho-Thr[172] of AMPKα (pAMPK) or total AMPKα (tAMPK). (B) Typical Western blots of cell extracts from H441 cells grown at the air–liquid interface, with or without pretreatment with STO609 and maintained at 21% O_2 (control) or exposed to 0.2% O_2 for 60 min and immunoblotted for phospho-Ser[79] of ACC (pACC), total ACC (tACC), phospho-Thr[172] of AMPKα (pAMPK) or total AMPKα (tAMPK). (C and D) Densitometry analysis of protein abundance pAMPK/ tAMPK and pACC/tACC from Western blots shown in (A) and (B). Results are shown as mean ± SEM. Significantly different from control: *$P < 0.05$ ($n = 3$). (E and F) A549 and H441cells grown in submerged culture maintained at 21% O_2 (control), or exposed to 3% O_2 for 60 min before or after pretreatment with STO609 prior to exposure to 3% O_2, fixed and immunostained for pAMPK. pAMPK was visualized with a Texas Red secondary antiserum. Nuclei are stained blue using DAPI.

lower than those at the air–liquid interface. This would explain why 3% O_2 activated AMPK in H441 cells grown in submerged culture and at the liquid–liquid interface. It would also explain our observation that AMPK was mildly activated when polarized epithelial cells at the liquid–liquid interface were exposed to normoxia (~21% O_2). In support of the latter findings, the addition of 5–10 mm depth of apical fluid was shown to elevate a number of hypoxic markers, including HIF1α, in human colonic HT29 cells grown as monolayers in normoxia (Guimbellot *et al.*, 2008). The changes in the peri-cellular PO_2 of submerged cultures are also likely to be more rapid in the face of a reduction rather than an increase in

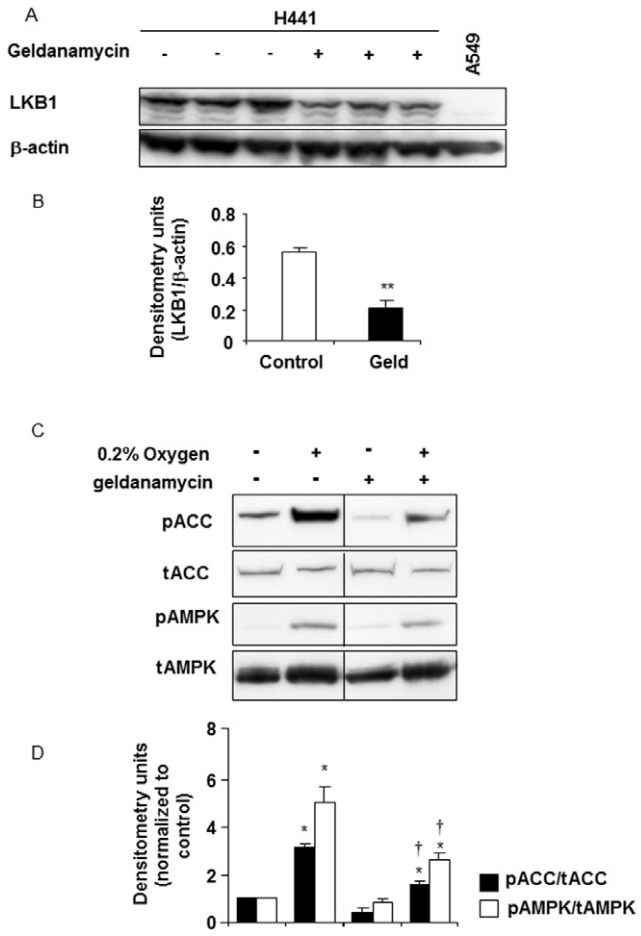

Figure 7

Effect of geldenamycin on activation of AMPK in H441 cells exposed to hypoxia. (A) Typical Western blot of cell extracts from H441 monolayers grown at the air–liquid interface before and after treatment with geldnamycin (10 μM for 24 h) immunoblotted for LKB1 or β-actin. A lane of cell extract from A549 cells (which do not contain LKB1) is shown to the right-hand side as a negative control. (B) Densitometry analysis of protein abundance LKB1/β-actin from Western blots shown in (A). *Significantly different from control: $P < 0.05$ ($n = 3$). (C) Typical Western blot of extracts from cells grown at the air–liquid interface pretreated with geldnamycin before exposure to 0.2% O_2 for 60 min and immunoblotted for phospho-Ser^{79} of ACC (pACC), total ACC (tACC), phospho-Thr^{172} of AMPKα (pAMPK) or total AMPKα (tAMPK). (These lanes were contained on the same gel shown in Figure 6C and utilize the same controls but have been presented as an independent figure for clarity). (D) Densitometry analysis of protein abundance pAMPK/tAMPK and pACC/tACC from Western blots as shown in (C). *Significantly different from control: $P < 0.05$ ($n = 4$). †Significantly different from untreated cells: $P < 0.05$ ($n = 4$).

gaseous PO_2 (Bambrick *et al.*, 2011). For example, the pericellular PO_2 of cultured A549 lung epithelial cells exposed to hypoxia decreased within 15 min (Allen *et al.*, 2001), consistent with the time course of activation we determined for AMPK. We cannot rule out the possibility that increased apical fluid volume may also alter other factors that could contribute to increased cellular stress [i.e. apical pressure, rapid activation of ENaC (Tan *et al.*, 2011)]. However, we suggest that apical fluid restricted diffusion of O_2 to the cell surface resulting in a lowering of PO_2 at the cell membrane and potentiation of the hypoxic effect, which led to energy restriction and an alteration of the cellular AMP : ATP ratio. A future study, utilizing oxygen electrodes to determine exactly the PO_2 at the cell membrane required to activate AMPK, would now be useful.

These findings are important because much work on respiratory cells has utilized cells grown in submerged culture to study effects of altered PO_2. We are proposing that this may not accurately reflect the normal *in vivo* conditions, which are more like those of cells grown at the air–liquid interface. Thus, in situations where lung apical fluid volume is increased (pulmonary oedema), more physiologically relevant levels of hypoxia could activate AMPK in lung epithelial cells.

There is mounting evidence that AMPK can be activated by hypoxic elevation of ROS in the absence of changes in the AMP : ATP ratio (Emerling *et al.*, 2009; Gusarova *et al.*, 2011). In addition, an elevation of intracellular Ca^{2+} leading to activation of CaMKKβ and phosphorylation of AMPK was shown to mediate the effects of hypoxia in A549 distal lung epithelial cells (Gusarova *et al.*, 2011). However, our data do not currently support these pathways in H441 airway cells. Under the conditions investigated, AMPK was not activated in the absence of a change in the AMP : ATP ratio. Furthermore, in monolayers grown at the liquid–liquid interface, AMPK was activated by both mild and extreme hypoxia, but neither of the ROS scavengers NAC or TEMPOL had any effect on the phosphorylation of AMPK or ACC. Moreover, although elevation of intracellular Ca^{2+} with ionomycin resulted in activation of AMPK via a STO609-sensitive pathway in H441 cells, hypoxia-induced phosphorylation of AMPK was not affected by this inhibitor. Conversely, hypoxic activation of AMPK in A549 cells was inhibited by STO609, consistent with the findings of Gusarova *et al.* (2011). Thus, these data indicate that ROS and CaMKK do not play a critical role in hypoxic activation of AMPK in H441 cells.

The reduction of LKB1 protein with geldenamycin suppressed the hypoxia-induced AMPK activity indicating that LKB1-mediated phosphorylation is the primary route for activation of AMPK. We were unable to completely inhibit hypoxic activation of AMPK using this method, probably because of the residual activity of the remaining LKB1 protein. We therefore propose that hypoxic activation of AMPK in H441 epithelial cells requires a change in the cellular AMP : ATP ratio and LKB1 activity. These results contrast with findings in A549 and type II alveolar epithelial cells (Gusarova *et al.*, 2011). This may reflect differences between the cell types, sensitivity to changes in PO_2 and the signalling pathways utilized in the distal lung versus the airway. It is important to note that A549 cells do not contain LKB1 and may therefore preferentially exploit alternative hypoxia-sensing pathways.

We showed for the first time that, under conditions where AMPK is activated, hypoxia (3% and 0.2% O_2) inhibits transepithelial $I_{amiloride}$, $I_{ouabain}$ and G_{Na+} across H441 airway epithelial cells. These findings are consistent with studies in human A549 and rat alveolar type II cells where exposure to hypoxia (1.5–3%) inhibited Na^+ transport processes (Heberlein *et al.*,

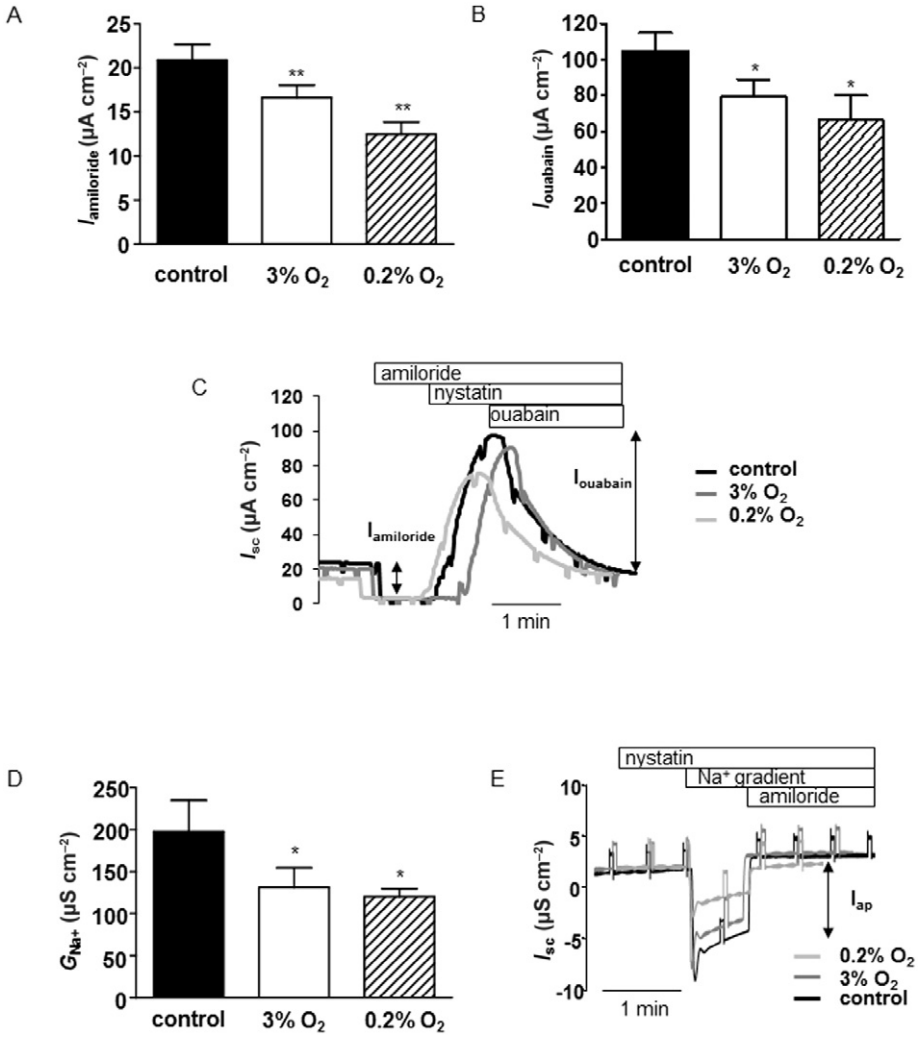

Figure 8

Effect of hypoxia on transepithelial $I_{amiloride}$, basolateral $I_{ouabain}$ and apical G_{Na+}. Cells grown at the liquid–liquid interface were maintained under 21% O_2 (control) or exposed to 3% or 0.2% O_2 for 60 min before being mounted in Ussing chambers. (A) Amiloride-sensitive transepithelial I_{sc} ($I_{amiloride}$). (B) Basolateral ouabain-sensitive I_{sc} ($I_{ouabain}$). (C) Typical current traces from which values for $I_{amiloride}$ and $I_{ouabain}$ were obtained. Spontaneous transepithelial I_{sc} was measured before the addition of amiloride (10 μM) to the apical bath over the time course shown in the box above the trace. Under the same recording conditions, nystatin (75 μM) was added to the apical chamber. When the current reached peak values, ouabain (1 mM) was added to the basolateral chamber. (D) Apical amiloride-sensitive Na^+ conductance (G_{Na+}). (E) Typical current traces showing spontaneous I_{sc} (in potassium gluconate solution) before the addition of nystatin to the basolateral bath over the time course shown in the box above the trace. A Na^+ gradient was then applied across the apical membrane as indicated, followed by the addition of amiloride (10 μM). G_{Na+} was calculated from the amiloride-sensitive apical current (I_{ap}). Significantly different from control: $^*P < 0.05$, $^{**}P < 0.01$ ($n = 4$).

2000; Wodopia *et al.*, 2000; Mairbaeurl *et al.*, 2002). Interestingly, transepithelial resistance was also increased in response to hypoxia. Similar changes in resistance have been associated with pharmacological activation of AMPK in H441 cells (Woollhead *et al.*, 2005; 2007; Mace *et al.*, 2008).

The effect of hypoxia on $I_{ouabain}$ was disrupted by the expression of a shRNA construct that reduced AMPK protein abundance in the cells. Furthermore, the expression of constitutively active α-AMPK inhibited $I_{ouabain}$ and prevented any further inhibition by hypoxia. These data indicate that hypoxic activation of AMPK inhibited Na^+K^+ ATPase in H441 cell monolayers. These findings are consistent with our previous observations that pharmacological activation of AMPK inhibits Na^+K^+ ATPase in H441 cells (Woollhead *et al.*, 2005; 2007; Albert *et al.*, 2008). Exposure to hypoxia (1.5% O_2) has also been shown to inhibit Na^+K^+ ATPase function in human A549 and rat alveolar type II cells via AMPK (Gusarova *et al.*, 2009). However, we were unable to inhibit the effect of hypoxia on apical G_{Na+} using such constructs, even though there is evidence that activation of AMPK inhibits apical G_{Na+} and ENaC channels in these and other epithelial cells (Carattino *et al.*, 2005; Woollhead *et al.*, 2005; 2007; Bhalla *et al.*,

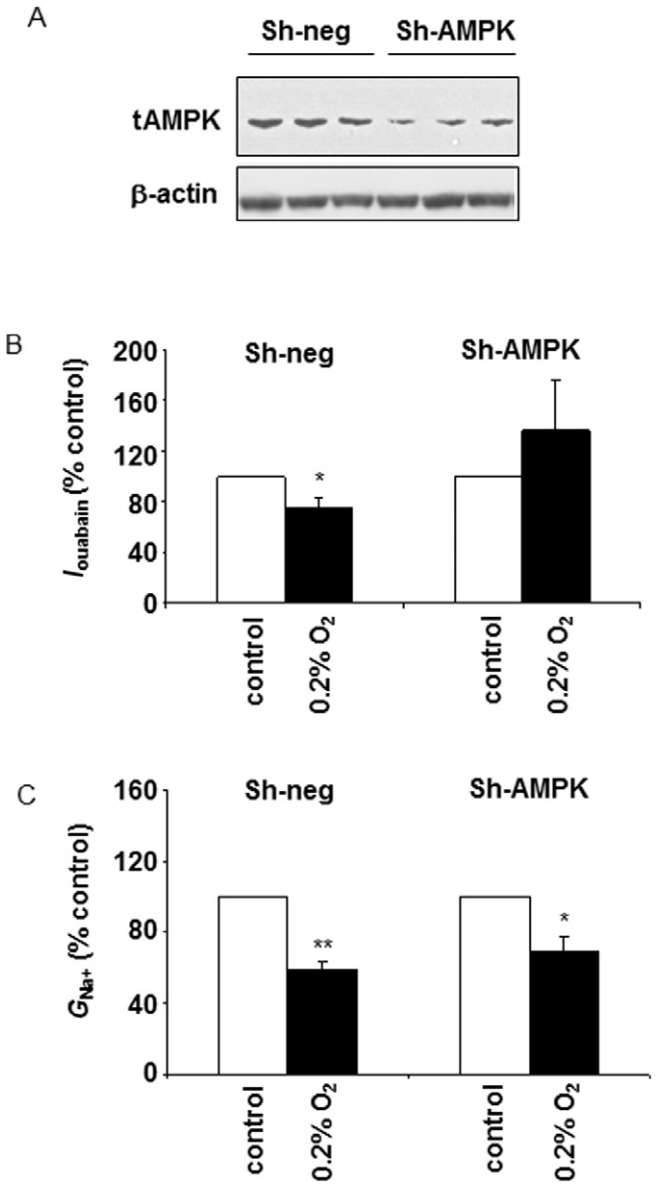

Figure 9

Effect of expression of Sh-neg and Sh-AMPK lentiviral vectors on $I_{ouabain}$ and G_{Na+} in H441 cells. (A) Western blot of total AMPK in cells grown at the air–liquid interface and transduced with Sh-neg or Sh-AMPK lentivector. (B) $I_{ouabain}$ in cells transduced with Sh-neg or Sh-AMPK lentivector maintained under 21% O_2 (control) or exposed to 0.2% O_2 for 60 min. (C) G_{Na+} in cells transduced with Sh-neg or Sh-AMPK lentivector maintained under 21% O_2 (control) or exposed to 0.2% O_2 for 60 min. Data are shown as % control for comparative purposes. Significantly different from control: *$P < 0.05$, **$P < 0.01$ ($n = 4$).

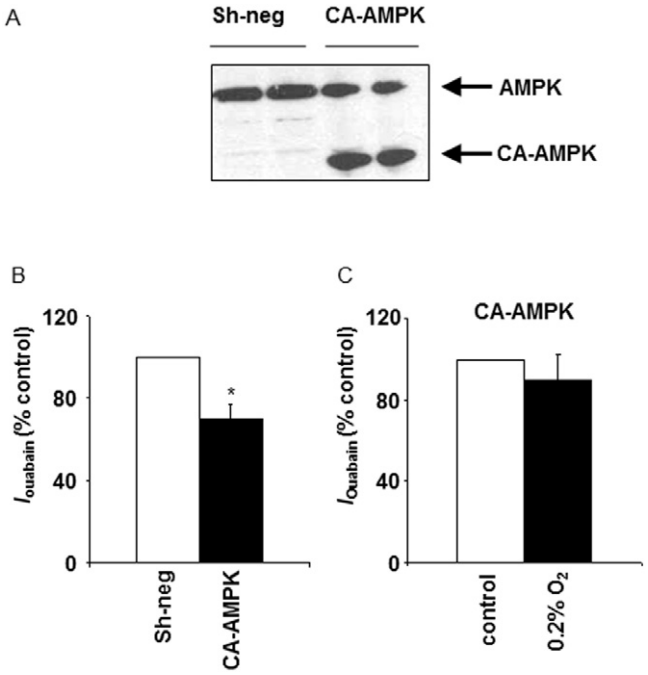

Figure 10

Effect of expression of CA-AMPK lentiviral vector on $I_{ouabain}$ in H441 cells. (A) Western blot of total AMPK in cells grown at the air–liquid interface and transduced with Sh-neg or CA-AMPK lentivector. CA-AMPK is a smaller protein of 36 kDa, which runs below the endogenous protein. (B) Transepithelial $I_{ouabain}$ in cells maintained at 21% O_2 and transduced with CA-AMPK compared to that of cells transduced with Sh-neg lentivector. Data are shown as % Sh-neg for comparative purposes. Significantly different from control *$P < 0.05$ ($n = 3$). (C) $I_{ouabain}$ in cells transduced with CA-AMPK lentivector maintained at 21% O_2 (control) or exposed to 0.2% O_2 for 60 min (for reference, the effect of 0.2% O_2 for 60 min on $I_{ouabain}$ in cells transduced with Sh-neg is shown in Figure 8C). Data are shown as % control for comparative purposes. *Significantly different from control: $P < 0.05$ ($n = 4$).

2006; Albert *et al.*, 2008). We cannot rule out the possibility that more prolonged exposure to hypoxia could elicit AMPK-mediated effects on apical channels. However, in renal collecting duct cells, pre-activation of AMPK with AICAR did not mitigate the inhibitory effect of hypoxia (8% O_2 for 24 h) on Na^+ transport, indicating that the apical response to hypoxia involves other AMPK-independent mechanisms (Husted *et al.*, 2011).

Hypoxia modifies intracellular ROS, and there is evidence that amiloride-sensitive ENaC channels are acutely regulated by ROS (Helms *et al.*, 2008; Althaus *et al.*, 2009; Yip *et al.*, 2010). That NAC did not prevent the hypoxic inhibition of apical G_{Na+} indicates that changes in H_2O_2 were not involved. However, both TEMPOL and apocynin prevented the effect of hypoxia on apical G_{Na+}, indicating a potential role for superoxide (O_2^-) in the hypoxic suppression of apical ENaC channel activity. TEMPOL is a scavenger of O_2^- that can be generated by a number of cellular sources including NADPH oxidase. In A6 renal cells, aldosterone elevation of intracellular O_2^- increased ENaC activity, which was abolished in the presence of TEMPOL (Yu *et al.*, 2007). This would be consistent with our finding that TEMPOL reduced G_{Na+} and prevented any further suppression of ENaC activity by hypoxia. Apocynin inhibits NADPH oxidase (NOX) activity in the plasma membrane, which is responsible for the generation of O_2^- from O_2, potentially providing a localized source of O_2^-

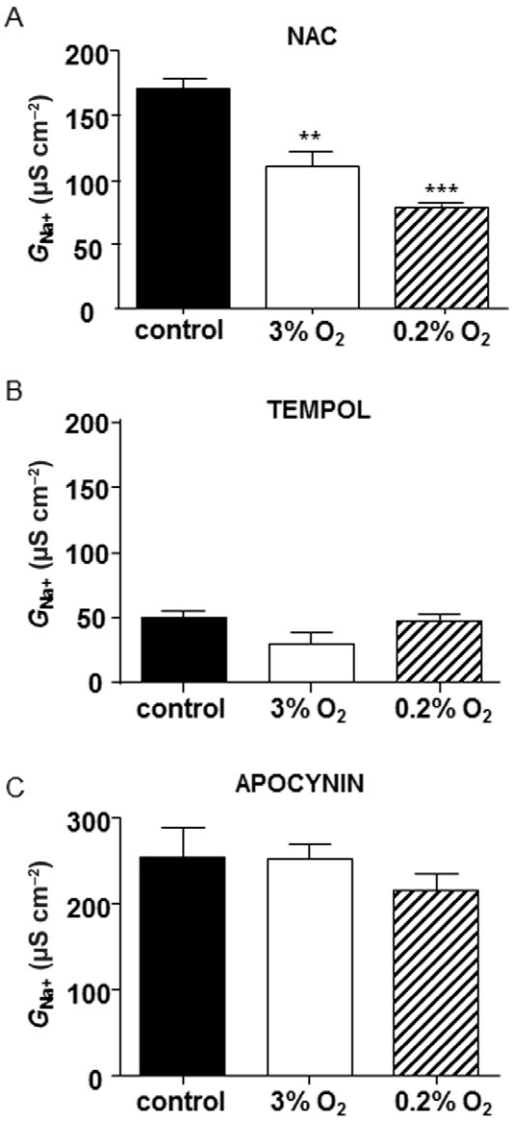

Figure 11

Effect of NAC, TEMPOL and apocynin on apical amiloride-sensitive G_{Na+}. Cells grown at the liquid–liquid interface were pretreated with NAC, TEMPOL or apocynin and maintained at 21% O_2 (control) or exposed to 3% or 0.2% hypoxia for 60 min. G_{Na+} was measured in basolaterally permeabilized monolayers after apical application of 10 μM amiloride. Significantly different from control: $^*P < 0.05$, $^{**}P < 0.01$, $^{***}P < 0.001$ ($n = 3$).

proximal to the Na^+ channel. Our data support the idea that when O_2 availability is reduced, the localized production of O_2^- by NOX is compromised, leading to a reduction in Na^+ channel activity. More work is now required to identify how hypoxia affects different sources of intracellular O_2^- and how these contribute to the regulation of apical Na^+ channels. In addition, O_2^- may not regulate ENaC channels directly. For example, O_2^- can sequester NO, which has been shown to inhibit ENaC channels (Althaus *et al.*, 2011; Husted *et al.*, 2011).

In conclusion, we have shown that a 60 min exposure to hypoxia activated AMPK in H441 airway epithelial cells. The sensitivity to hypoxia was increased by the addition of fluid to the apical surface of cell monolayers grown at the air–liquid interface, which may have important consequences in lung disease conditions. Activation of AMPK was associated with an elevation of the cellular AMP : ATP ratio and the presence of the upstream kinase LKB1. Hypoxia inhibited amiloride-sensitive transepithelial Na^+ transport by inhibiting both basolateral Na^+K^+ ATPase and apical amiloride-sensitive Na^+ channel activity. However, the signalling pathways regulating apical and basolateral responses to hypoxia were different. AMPK mediated the effect of hypoxia on Na^+K^+ ATPase, but the effect on apical Na^+ channels involved the action of superoxide O_2^-. Therefore, we propose that hypoxia simultaneously activates AMPK-dependent and -independent pathways to decrease transepithelial Na^+ transport in polarized H441 airway epithelial cells.

Acknowledgements

This work was funded by Biotechnology and Biological Sciences Research Council Project Grant BB/E013597/1, Wellcome Trust Project Grant PG/07/079/23568 and St George's University of London (to DLB) and the 7th EU Framework Programme (PERSIST project, grant agreement no. 222878, to RJY-M). MIH is a British Heart Foundation Intermediate Basic Science Research Fellow (FS/06/077).

Conflicts of Interest

None.

References

Abramov AY, Duchen MR (2003). Actions of ionomycin, 4-BrA23187 and a novel electrogenic Ca2+ ionophore on mitochondria in intact cells. Cell Calcium 33: 101–112.

Albert AP, Woollhead AM, Mace OJ, Baines DL (2008). AICAR decreases the activity of two distinct amiloride-sensitive Na+-permeable channels in H441 human lung epithelial cell monolayers. Am J Physiol Lung Cell Mol Physiol 295: L837–L848.

Allen CB, Schneider BK, White CW (2001). Limitations to oxygen diffusion and equilibration in in vitro cell exposure systems in hyperoxia and hypoxia. Am J Physiol Lung Cell Mol Physiol 281: L1021–L1027.

Althaus M, Fronius M, Buchackert Y, Vadasz I, Clauss WG, Seeger W *et al.* (2009). Carbon monoxide rapidly impairs alveolar fluid clearance by inhibiting epithelial sodium channels. Am J Respir Cell Mol Biol 41: 639–650.

Althaus M, Pichl A, Clauss WG, Seeger W, Fronius M, Morty RE (2011). Nitric oxide inhibits highly selective sodium channels and the Na+/K+-ATPase in H441 Cells. Am J Respir Cell Mol Biol 44: 53–65.

Bambrick LL, Kostov Y, Rao G (2011). In vitro cell culture pO(2) is significantly different from incubator pO(2). Biotechnol Prog 27: 1–2.

Bhalla V, Oyster NM, Fitch AC, Wijngaarden MA, Neumann D, Schlattner U *et al.* (2006). AMP-activated kinase inhibits the epithelial Na+ channel through functional regulation of the ubiquitin ligase Nedd4-2. J Biol Chem 281: 26159–26169.

Carattino MD, Edinger RS, Grieser HJ, Wise R, Neumann D, Schlattner U *et al.* (2005). Epithelial sodium channel inhibition by AMP-activated protein kinase in oocytes and polarized renal epithelial cells. J Biol Chem 280: 17608–17616.

Clair C, Chalumeau C, Tordjmann T, Poggioli J, Erneux C, Dupont G *et al.* (2001). Investigation of the roles of Ca(2+) and InsP(3) diffusion in the coordination of Ca(2+) signals between connected hepatocytes. J Cell Sci 114: 1999–2007.

Collett A, Ramminger SJ, Olver RE, Wilson SM (2002). Beta-adrenoceptor-mediated control of apical membrane conductive properties in fetal distal lung epithelia. Am J Physiol Lung Cell Mol Physiol 282: L621–L630.

Dada LA, Sznajder JI (2007). Hypoxic inhibition of alveolar fluid reabsorption. Adv Exp Med Biol 618: 159–168.

Dada LA, Chandel NS, Ridge KM, Pedemonte C, Bertorello AM, Sznajder JI (2003). Hypoxia-induced endocytosis of Na,K-ATPase in alveolar epithelial cells is mediated by mitochondrial reactive oxygen species and PKC-zeta. J Clin Invest 111: 1057–1064.

Dull T, Zufferey R, Kelly M, Mandel RJ, Nguyen M, Trono D *et al.* (1998). A third-generation lentivirus vector with a conditional packaging system. J Virol 72: 8463–8471.

Emerling BM, Weinberg F, Snyder C, Burgess Z, Mutlu GM, Viollet B *et al.* (2009). Hypoxic activation of AMPK is dependent on mitochondrial ROS but independent of an increase in AMP/ATP ratio. Free Radic Biol Med 46: 1386–1391.

Evans AM, Mustard KJ, Wyatt CN, Peers C, Dipp M, Kumar P *et al.* (2005). Does AMP-activated protein kinase couple inhibition of mitochondrial oxidative phosphorylation by hypoxia to calcium signaling in O2-sensing cells? J Biol Chem 280: 41504–41511.

Guimbellot JS, Fortenberry JA, Siegal GP, Moore B, Wen H, Venglarik C *et al.* (2008). Role of oxygen availability in CFTR expression and function. Am J Respir Cell Mol Biol 39: 514–521.

Guney S, Schuler A, Ott A, Hoschele S, Zugel S, Baloglu E *et al.* (2007). Dexamethasone prevents transport inhibition by hypoxia in rat lung and alveolar epithelial cells by stimulating activity and expression of Na+-K+-ATPase and epithelial Na+ channels. Am J Physiol Lung Cell Mol Physiol 293: L1332–L1338.

Gusarova GA, Dada LA, Kelly AM, Brodie C, Witters LA, Chandel NS *et al.* (2009). Alpha1-AMP-activated protein kinase regulates hypoxia-induced Na,K-ATPase endocytosis via direct phosphorylation of protein kinase C zeta. Mol Cell Biol 29: 3455–3464.

Gusarova GA, Trejo HE, Dada LA, Briva A, Welch LC, Hamanaka RB *et al.* (2011). Hypoxia Leads to Na,K-ATPase Downregulation via Ca2+ Release-Activated Ca2+ Channels and AMPK Activation. Mol Cell Biol 31: 3546–3556.

Hardie DG, Sakamoto K (2006). AMPK: a key sensor of fuel and energy status in skeletal muscle. Physiology (Bethesda) 21: 48–60.

Harhun M, Gordienko D, Kryshtal D, Pucovsky V, Bolton T (2006). Role of intracellular stores in the regulation of rhythmical [Ca2+]i changes in interstitial cells of Cajal from rabbit portal vein. Cell Calcium 40: 287–298.

Hawley SA, Davison M, Woods A, Davies SP, Beri RK, Carling D *et al.* (1996). Characterization of the AMP-activated protein kinase kinase from rat liver and identification of threonine 172 as the major site at which it phosphorylates AMP-activated protein kinase. J Biol Chem 271: 27879–27887.

Hawley SA, Pan DA, Mustard KJ, Ross L, Bain J, Edelman AM *et al.* (2005). Calmodulin-dependent protein kinase kinase-beta is an alternative upstream kinase for AMP-activated protein kinase. Cell Metab 2: 9–19.

Heberlein W, Wodopia R, Bartsch P, Mairbaurl H (2000). Possible role of ROS as mediators of hypoxia-induced ion transport inhibition of alveolar epithelial cells. Am J Physiol 278: L640–L648.

Helms MN, Jain L, Self JL, Eaton DC (2008). Redox regulation of epithelial sodium channels examined in alveolar type 1 and 2 cells patch-clamped in lung slice tissue. J Biol Chem 283: 22875–22883.

Hummler E, Baker P, Gatzy J, Berrmann F, Verdumo C, Schmidt A *et al.* (1996). Early death due to defective neonatal lung liquid clearance in aENaC-deficient mice. Nat Genet 12: 325–328.

Husted RF, Lu H, Sigmund RD, Stokes JB (2011). Oxygen regulation of the epithelial Na channel in the collecting duct. Am J Physiol Renal Physiol 300: F412–F424.

Liu C, Hermann TE (1978). Characterization of ionomycin as a calcium ionophore. J Biol Chem 253: 5892–5894.

Lynn SG, LaPres JJ, Studer-Rabeler K (2011). Oxygen monitoring in cell cultures. Genetic Engineering & Biotechnology News 31: 1–2.

McAlroy HL, Ahmed S, Day SM, Baines DL, Wong HY, Yip CY *et al.* (2000). Multiple P2Y receptor subtypes in the apical membranes of polarized epithelial cells. Br J Pharmacol 131: 1651–1658.

Mace OJ, Woollhead AM, Baines DL (2008). AICAR activates AMPK and alters PIP2 association with ENaC to inhibit Na+ transport in H441 lung epithelial cells. J Physiol 586: 4541–4557.

Mairbaeurl H, Mayer K, Kim K-J, Borok Z, Baertsch P, Crandall ED (2002). Hypoxia decreases active Na transport across primary rat alveolar epithelial cell monolayers. Am J Physiol Lung Cell Mol Physiol 282: L659–L665.

Mairbaurl H (2006). Role of alveolar epithelial sodium transport in high altitude pulmonary edema (HAPE). Respir Physiol Neurobiol 151: 178–191.

Mairbaurl H, Wodopia R, Eckes S, Schulz S, Bartsch P (1997). Impairment of cation transport in A549 cells and rat alveolar epithelial cells by hypoxia. Am J Physiol 273: L797–L806.

Marley AE, Sullivan JE, Carling D, Abbott WM, Smith GJ, Taylor IW *et al.* (1996). Biochemical characterization and deletion analysis of recombinant human protein phosphatase 2C alpha. Biochem J 320: 801–806.

Metzen E, Wolff M, Fandrey J, Jelkmann W (1995). Pericellular PO2 and O2 consumption in monolayer cell cultures. Respir Physiol 100: 101–106.

Momcilovic M, Hong SP, Carlson M (2006). Mammalian TAK1 activates Snf1 protein kinase in yeast and phosphorylates AMP-activated protein kinase in vitro. J Biol Chem 281: 25336–25343.

Mortimer H, Patel S, Peacock AJ (2004). The genetic basis of high-altitude pulmonary oedema. Pharmacol Ther 101: 183–192.

Myerburg MM, King JJD, Oyster NM, Fitch AC, Magill A, Baty CJ *et al.* (2010). AMPK agonists ameliorate sodium and fluid transport and inflammation in CF airway epithelial cells. Am J Respir Cell Mol Biol 42: 676–684.

Nofziger C, Brown KK, Smith CD, Harrington W, Murray D, Bisi J *et al.* (2009). PPARgamma agonists inhibit vasopressin-mediated anion transport in the MDCK-C7 cell line. Am J Physiol Renal Physiol 297: F55–F62.

Nony P, Gaude H, Rossel M, Fournier L, Rouault JP, Billaud M (2003). Stability of the Peutz-Jeghers syndrome kinase LKB1 requires its binding to the molecular chaperones Hsp90/Cdc37. Oncogene 22: 9165–9175.

Planes C, Escoubet B, Blot-Chabaud M, Friedlander G, Farman N, Clerici C (1997). Hypoxia downregulates expression and activity of epithelial sodium channels in rat alveolar epithelial cells. Am J Respir Cell Mol Biol 17: 508–518.

Planes C, Blot-Chabaud M, Matthay MA, Couette S, Uchida T, Clerici C (2002). Hypoxia and beta 2-agonists regulate cell surface expression of the epithelial sodium channel in native alveolar epithelial cells. J Biol Chem 277: 47318–47324.

Ramminger SJ, Baines DL, Olver RE, Wilson SM (2000). The effects of P_{O2} upon transepithelial ion transport in fetal rat distal lung epithelial cells. J Physiol 524.2: 539–547.

Richard K, Ramminger SJ, Forsyth L, Burchell A, Wilson SM (2004). Thyroid hormone potentiates glucocorticoid-evoked airway Na+ transport without affecting alpha-ENaC transcription. FEBS Lett 576: 339–342.

Sartori C, Allemann Y, Duplain H, Lepori M, Egli M, Lipp E *et al.* (2002). Salmeterol for the prevention of high-altitude pulmonary edema. N Engl J Med 346: 1631–1636.

Sutherland CM, Hawley SA, McCartney RR, Leech A, Stark MJ, Schmidt MC *et al.* (2003). Elm1p is one of three upstream kinases for the Saccharomyces cerevisiae SNF1 complex. Curr Biol 13: 1299–1305.

Tan CD, Selvanathar IA, Baines DL (2011). Cleavage of endogenous gammaENaC and elevated abundance of alphaENaC are associated with increased Na(+) transport in response to apical fluid volume expansion in human H441 airway epithelial cells. Pflugers Arch 462: 431–441.

Tarran R (2008). Raising the volume on near-silent epithelial Na+ channels. J Physiol 586: 4583–4584.

Verhoeven AJ, Woods A, Brennan CH, Hawley SA, Hardie DG, Scott J *et al.* (1995). The AMP-activated protein kinase gene is highly expressed in rat skeletal muscle. Alternative splicing and tissue distribution of the mRNA. Eur J Biochem 228: 236–243.

Widdicombe JH (2002). Regulation of the depth and composition of airway surface liquid. J Anat 201: 313–318.

Wilson WA, Hawley SA, Hardie DG (1996). Glucose repression/derepression in budding yeast: SNF1 protein kinase is activated by phosphorylation under derepressing conditions, and this correlates with a high AMP:ATP ratio. Curr Biol 6: 1426–1434.

Winder WW, Wilson HA, Hardie DG, Rasmussen BB, Hutber CA, Call GB *et al.* (1997). Phosphorylation of rat muscle acetyl-CoA carboxylase by AMP-activated protein kinase and protein kinase A. J Appl Physiol 82: 219–225.

Wodopia R, Ko HS, Billian J, Wiesner R, Bartsch P, Mairbaurl H (2000). Hypoxia decreases proteins involved in epithelial electrolyte transport in A549 cells and rat lung. Am J Physiol Lung Cell Mol Physiol 279: L1110–L1119.

Woods A, Johnstone SR, Dickerson K, Leiper FC, Fryer LG, Neumann D *et al.* (2003). LKB1 is the upstream kinase in the AMP-activated protein kinase cascade. Curr Biol 13: 2004–2008.

Woods A, Dickerson K, Heath R, Hong SP, Momcilovic M, Johnstone SR *et al.* (2005). Ca2+/calmodulin-dependent protein kinase kinase-beta acts upstream of AMP-activated protein kinase in mammalian cells. Cell Metab 2: 21–33.

Woollhead AM, Scott JW, Hardie DG, Baines DL (2005). Phenformin and 5-aminoimidazole-4-carboxamide-1-{beta}-D-ribofuranoside (AICAR) activation of AMP-activated protein kinase inhibits transepithelial Na+ transport across H441 lung cells. J Physiol 566: 781–792.

Woollhead AM, Sivagnanasundaram J, Kalsi KK, Pucovsky V, Pellatt LJ, Scott JW *et al.* (2007). Pharmacological activators of AMP-activated protein kinase have different effects on Na(+) transport processes across human lung epithelial cells. Br J Pharmacol 151: 1204–1215.

Wyatt CN, Mustard KJ, Pearson SA, Dallas ML, Atkinson L, Kumar P *et al.* (2007). AMP-activated protein kinase mediates carotid body excitation by hypoxia. J Biol Chem 282: 8092–8098.

Xie Z, Dong Y, Zhang M, Cui MZ, Cohen RA, Riek U *et al.* (2006). Activation of protein kinase C zeta by peroxynitrite regulates LKB1-dependent AMP-activated protein kinase in cultured endothelial cells. J Biol Chem 281: 6366–6375.

Yanez-Munoz RJ, Balaggan KS, MacNeil A, Howe SJ, Schmidt M, Smith AJ *et al.* (2006). Effective gene therapy with nonintegrating lentiviral vectors. Nat Med 12: 348–353.

Yip YL, Tsang CM, Deng W, Cheung PY, Jin Y, Cheung AL *et al.* (2010). Expression of Epstein-Barr virus-encoded LMP1 and hTERT extends the life span and immortalizes primary cultures of nasopharyngeal epithelial cells. J Med Virol 82: 1711–1723.

Yu L, Bao HF, Self JL, Eaton DC, Helms MN (2007). Aldosterone-induced increases in superoxide production counters nitric oxide inhibition of epithelial Na channel activity in A6 distal nephron cells. Am J Physiol Renal Physiol 293: F1666–F1677.

Zhao W, Wu J, Zhong L, Srivastava A (2007). Adeno-associated virus 2-mediated gene transfer: role of a cellular serine/threonine protein phosphatase in augmenting transduction efficiency. Gene Ther 14: 545–550.

Zhou G, Dada LA, Sznajder JI (2008). Regulation of alveolar epithelial function by hypoxia. Eur Respir J 31: 1107–1113.

Zufferey R, Dull T, Mandel RJ, Bukovsky A, Quiroz D, Naldini L *et al.* (1998). Self-inactivating lentivirus vector for safe and efficient in vivo gene delivery. J Virol 72: 9873–9880.